

LIE DERIVATIVE DISCRETIZATION SCHEME FOR SOLVING VARIABLE MASS SYSTEMS

Xinyue Jia¹  [0009-0007-1326-3562], Chang Liu¹  [0000-0001-8994-2579] and Wenan Jiang^{2*}  [0009-0008-4137-2827]

¹ College of Physics, Liaoning University, Shenyang, China

e-mail: xy15633606397@foxmail.com, changliu@lnu.edu.cn

² Faculty of Civil Engineering and Mechanics, Jiangsu University, Zhenjiang, China

e-mail: wajiang@ujs.edu.cn

*corresponding author

Abstract

Lie derivative plays a key role in mathematics and physics. In particular, the Lie derivative discretization scheme has been implemented for a relatively large time step in order to quickly solve the numerical solution of the system. In this paper, an algorithm of the Lie derivative discretization scheme is applied to variable mass systems. Four different types of variable mass systems are employed to study the numerical solutions, and the calculated results are consistent with those obtained by the fourth-order Runge-Kutta method. Computational experiments demonstrate the success of the proposed method on variable mass systems. Moreover, the algorithm of Lie derivative discretization is shown to have superior computational efficiency and larger time steps compared to the Runge-Kutta algorithm.

Keywords: variable mass, Lie derivative, discretization, high efficiency, large time step.

1. Introduction

Traditional system dynamics often assume that the system's mass is constant, but in practical application, there are many cases where mass is varying (Cveticanin 2016; Cao et al. 2023). Therefore, to describe and analyze the dynamic behavior of this kind of system more accurately, it is necessary to introduce the concept of a variable mass system. The study of variable mass systems has become a prominent area. The development of variable mass systems has been comprehensively and thoroughly reviewed (Irschik and Holl 2004; Cveticanin 2012). In the specific research within this field, investigations into the dynamic buckling phenomena of variable mass systems have been carried out (Cveticanin 2001), and detailed research and analysis have also been conducted on the vibration characteristics of linear variable mass single-degree-of-freedom systems (Flores et al. 2003). In the realm of equation formulation, a general governing equation has been successfully proffered by merging two independent equations that are typically employed to delineate single-degree-of-freedom free vibration systems with varying parameters (Nhleko 2009). Additionally, the generation of the motion control equation constitutes one of the notable achievements of the research (Hurtado 2018). Concurrently, extensive deliberations have also been conducted on effective methods for describing the dynamic behavior of time-varying

mass systems (Chen et al. 2024). Typically, obtaining precise solutions for differential equations with coefficients that change with time is challenging. Therefore, to get high-precision results, many numerical methods are usually used to find numerical solutions.

Researchers often use the algorithm of Lie discretization to solve simultaneous equations. It has superiority because it preserves the original equations' stationary points and covers large time steps. The truncated Lie derivative expansion scheme was proposed based on the original equation (Monaco and Normand-Cyrot 1990). It was verified through research that the derivative scheme of Lie retains the original fixed point (Mendes and Billings 2002), and it was also found that some solutions of the Lie derivative discretization method are topologically equivalent to the original system (Mendes and Letellier 2004). Regarding the Lie derivative discretization algorithm, research on chaotic behavior has been carried out (Letellier et al. 2007). Meanwhile, the discretization technology based on Taylor-Lee was proposed (Meena and Janardhanan 2018). In addition, a new approach was constructed through infinite computer arithmetic to calculate the Lie derivative of functions that cannot be expressed analytically (Iavernaro et al. 2021). Furthermore, in specific contexts such as in slow excitation shape memory oscillators, the Lie derivative algorithm was used to validate the outcomes of the Runge-Kutta method (Zhang et al. 2022). In the field of fluid mechanics, the Lie derivative was applied, and some conservation properties were obtained (Gouin 2023). The discretization scheme of the Lie derivative mentioned above mainly aims at mass invariant systems. But, for mass variable systems, the report is scarce. To address this issue, this paper studies the discretization algorithm of the Lie derivative for dynamical systems with variable mass. Section 2 provides the discretization algorithm for the Lie derivative of nonautonomous nonlinear systems. In the third section, the Lie derivative discretization algorithm is applied to four types of variable-mass systems, and the calculation results are compared with those of the traditional classical fourth-order Runge-Kutta algorithm. The fourth section is the conclusion of this paper.

2. Lie derivative discretization of mass-variable systems

We consider the forced vibration of a nonlinear oscillator with varying mass and the general model of the governing equation as:

$$m\ddot{x} - \dot{m}(u - \dot{x}) + c\dot{x} + q(x) = f \cos(\omega t) \quad (1)$$

where variable mass $m = m_0(1 + \alpha t)$ is a time-varying function, m_0 is an initial constant mass, α is the coefficient of continual mass variation, x is the displacement response of the system, c is the damping coefficient, u is the velocity after the mass change, $q(x)$ is a conservative restoring force, ω is the external excitation frequency and f is the external excitation amplitude.

Eq. (1) can be written as the general form:

$$\dot{\mathbf{x}} = \mathbf{g}(\mathbf{x}, t) \quad (2)$$

where $\mathbf{x} = [x_1, x_2]$, $x_1 = x$, $x_2 = \dot{x}$, then $g_1(\mathbf{x}, t) = x_2$, $g_2(\mathbf{x}, t) = \frac{\dot{m}(u - \dot{x}) - c\dot{x} - q(x) + f \cos(\omega t)}{m}$.

The mass-variable system (1) is generally a nonlinear equation with variable coefficients, so it is difficult to find the analytical solution. Thus, it is an effective approach to find the numerical solution. In order to obtain the numerical solutions, we will use the discretization scheme based on a Lie expansion of Eq. (2), which can be written as

$$\mathbf{x}_{k+1} = \mathbf{x}_k + \sum_{n=1}^{\eta} \frac{h^n}{n!} L_{\mathbf{g}}^n(t_k, \mathbf{x}_k) \quad (3)$$

where h represents the time size, and η represents the truncation order. The expression for the Lie derivative is

$$L_{\mathbf{g}}(t_k, \mathbf{x}_k) = \sum_{j=1}^m g_j(t_k, \mathbf{x}_k) \frac{\partial \mathbf{x}}{\partial x_j} \quad (4)$$

where g_j represents the j th component function of \mathbf{g} . The high-order Lie derivative can be expressed as

$$L_{\mathbf{g}}^n(t_k, \mathbf{x}_k) = L_{\mathbf{g}}(L_{\mathbf{g}}^{n-1}(t_k, \mathbf{x}_k)) \quad (5)$$

3. Numerical experiments

In order to express the excellent efficiency of the Lie derivative discretization scheme to several nonlinear oscillators with varying mass, we choose the traditional classical fourth-order Runge-Kutta algorithm for comparison to check the efficiency of the proposed method. Four oscillators with varying mass are carried out to show the efficiency of the new proposed scheme.

3.1 Variable mass monostable nonlinear oscillator

Firstly, a variable mass monostable nonlinear oscillator is introduced, and the motion equation is

$$m_0(1 + \alpha t)\ddot{x}(t) + (m_0\alpha + c)\dot{x}(t) + x(t) + x^3(t) = f \cos(\omega t) \quad (6)$$

with the initial conditions $x(0) = s_0, \dot{x}(0) = v_0$.

The discretization formula of the Lie derivative is applied to the Eq. (6), and its second-order discretization can be expressed as

$$\begin{aligned} x_{k+1} &= x_k + hL_{g_1}^1(t_k, x_k, y_k) + \frac{h^2}{2} L_{g_1}^2(t_k, x_k, y_k), \\ y_{k+1} &= y_k + hL_{g_2}^1(t_k, x_k, y_k) + \frac{h^2}{2} L_{g_2}^2(t_k, x_k, y_k), \end{aligned} \quad (7)$$

where

$$\begin{aligned} L_{g_1}^1(t_k, x_k, y_k) &= y_k, t_{k+1} = t_k + h, \\ L_{g_1}^2(t_k, x_k, y_k) &= -\frac{m_0\alpha + c}{m_0(1 + \alpha t)} y_k - \frac{1}{m_0(1 + \alpha t)} x_k - \frac{1}{m_0(1 + \alpha t)} x_k^3 + \frac{f \cos(\omega t)}{m_0(1 + \alpha t)}, \\ L_{g_2}^1(t_k, x_k, y_k) &= -\frac{m_0\alpha + c}{m_0(1 + \alpha t)} y_k - \frac{1}{m_0(1 + \alpha t)} x_k - \frac{1}{m_0(1 + \alpha t)} x_k^3 + \frac{f \cos(\omega t)}{m_0(1 + \alpha t)}, \\ L_{g_2}^2(t_k, x_k, y_k) &= \left[-\frac{1}{m_0(1 + \alpha t)} - \frac{3}{m_0(1 + \alpha t)} x_k^2 \right] y_k - \frac{m_0\alpha + c}{m_0(1 + \alpha t)} L_{g_2}^1(t_k, x_k, y_k). \end{aligned}$$

Fig. 1 shows the restoring force and potential energy function curves of the system (6). As can be seen from Fig. 1(a), when the restoring force is equal to 0, the function has only one

solution at $x = 0$. It is evident from Fig. 1(b) that the corresponding potential energy has a minimum value only at $x = 0$, so this point is stable and the potential has a single well, then the system is monostable.

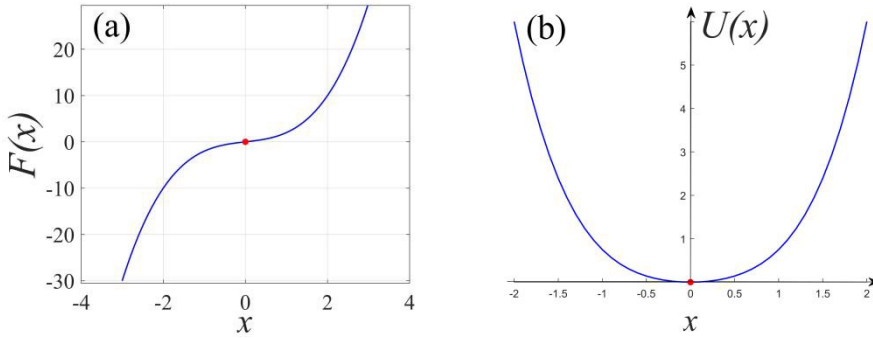


Fig. 1. The restoring force function curve (a) and the potential energy function curve (b) of the variable mass monostable nonlinear oscillator (The red dot indicates a stable static equilibrium point).

Fig. 2 shows the displacement response, 3D waveform, and phase diagram under three different excitation conditions, in which the blue line is the calculation result of the Lie derivative numerical algorithm and the red point is the result of the Runge-Kutta fourth-order algorithm. The fixed time step is 0.01. It is clear from the comparison diagram that the numerical results of the Lie derivative discretization algorithm are consistent with those of the fourth-order Runge-Kutta algorithm. Meanwhile, Table 1 displays the computational cost. As it can be seen from the table, when the time steps are the same, the calculation time can be significantly shortened by applying the Lie derivative algorithm, and the calculation efficiency can be improved to 93.7%.

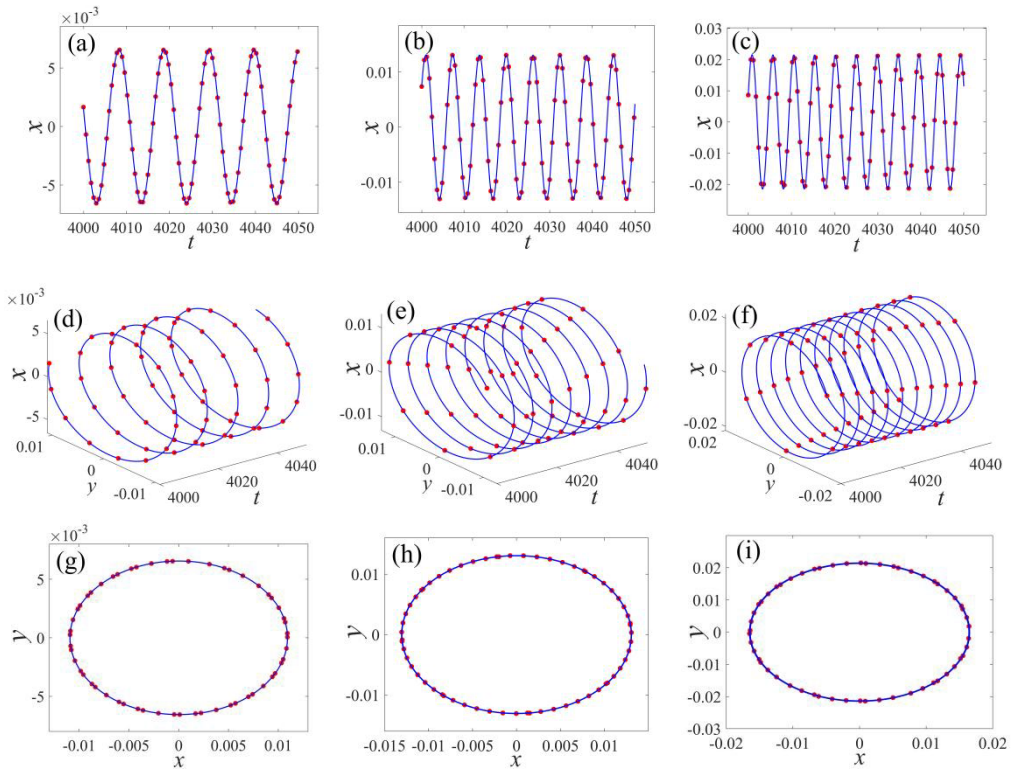


Fig. 2. The displacement response, 3D diagram, and phase diagram of the variable mass monostable nonlinear oscillator for (a, d, g) where $\omega = 0.6$, $f = 0.01$, (b, e, h) where $\omega = 1$, $f = 0.01$, (c, f, i) where $\omega = 1.3$, $f = 0.01$ (The blue line is the calculation result of the Lie derivative algorithm, and the red point is the calculation result of the Runge-Kutta fourth-order algorithm).

Fig. 3 compares the fourth-order Runge-Kutta algorithm (step size of 0.01) with the Lie derivative numerical algorithm (step size of 0.1). From the comparison diagram, we can see that the discretization algorithm of the Lie derivative has a satisfactory solution, and the calculation results of the two algorithms are in good agreement.

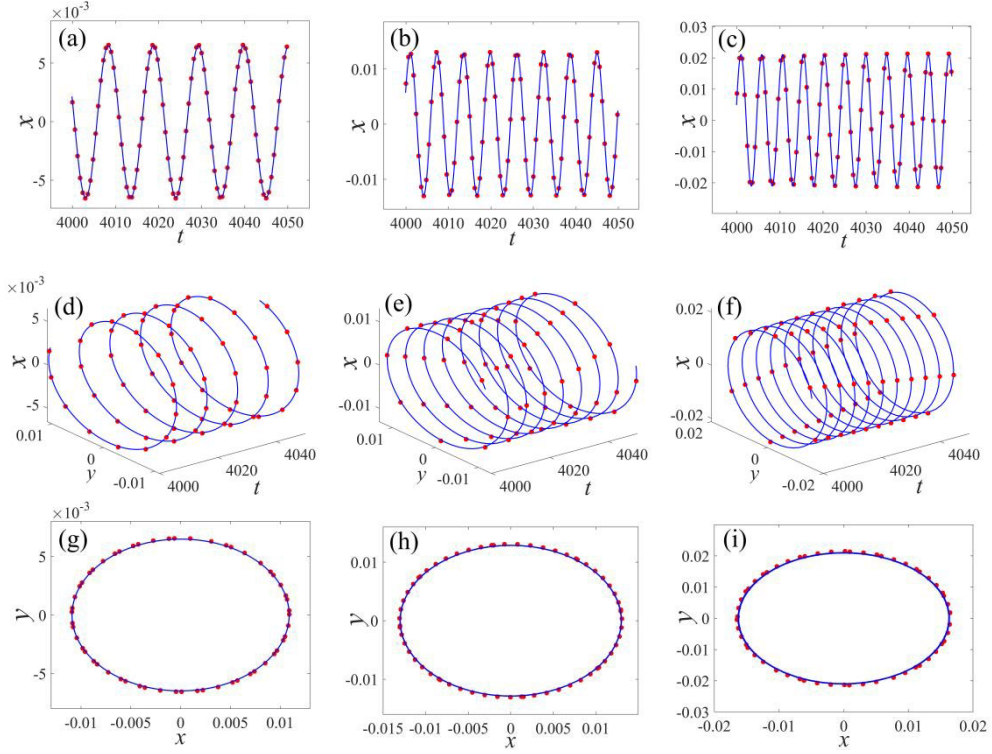


Fig. 3. The displacement response, 3D diagram, and phase diagram of the variable mass monostable nonlinear oscillator for (a, d, g) where $\omega = 0.6, f = 0.01$, (b, e, h) where $\omega = 1, f = 0.01$, (c, f, i) where $\omega = 1.3, f = 0.01$ (The blue line is the calculation result of the Lie derivative algorithm, and the red point is the calculation result of the fourth-order Runge-Kutta algorithm).

Fig. Method	Fig.2(a)	Fig.2(b)	Fig.2(c)
Lie	0.1562	0.1286	0.1178
Ode45	1.8325	1.8407	1.8687

Table 1. The computational cost of the two numerical schemes from the system (6)

3.2 Variable mass symmetric bistable nonlinear oscillator

Secondly, the variable mass symmetric bistable nonlinear oscillator is introduced, and the governing equation is

$$m_0(1 + \alpha t)\ddot{x}(t) + (m_0\alpha + c)\dot{x}(t) - x(t) + x^3(t) = f \cos(\omega t) \quad (8)$$

The discretization formula of the Lie derivative is applied to Eq. (8) of the variable mass symmetric bistable nonlinear oscillator, and its second-order discretization can be employed as

$$\begin{aligned}x_{k+1} &= x_k + hL_{g_1}^1(t_k, x_k, y_k) + \frac{h^2}{2}L_{g_1}^2(t_k, x_k, y_k), \\y_{k+1} &= y_k + hL_{g_2}^1(t_k, x_k, y_k) + \frac{h^2}{2}L_{g_2}^2(t_k, x_k, y_k),\end{aligned}\quad (9)$$

where

$$\begin{aligned}L_{g_1}^1(t_k, x_k, y_k) &= y_k, t_{k+1} = t_k + h, \\L_{g_1}^2(t_k, x_k, y_k) &= -\frac{m_0\alpha + c}{m_0(1+\alpha t)}y_k + \frac{1}{m_0(1+\alpha t)}x_k - \frac{1}{m_0(1+\alpha t)}x_k^3 + \frac{f \cos(\omega t)}{m_0(1+\alpha t)}, \\L_{g_2}^1(t_k, x_k, y_k) &= -\frac{m_0\alpha + c}{m_0(1+\alpha t)}y_k + \frac{1}{m_0(1+\alpha t)}x_k - \frac{1}{m_0(1+\alpha t)}x_k^3 + \frac{f \cos(\omega t)}{m_0(1+\alpha t)}, \\L_{g_2}^2(t_k, x_k, y_k) &= \left[\frac{1}{m_0(1+\alpha t)} - \frac{3}{m_0(1+\alpha t)}x_k^2 \right]y_k - \frac{m_0\alpha + c}{m_0(1+\alpha t)}L_{g_2}^1(t_k, x_k, y_k).\end{aligned}$$

Fig. 4 shows the restoring force and potential energy function curves. Fig. 4(a) displays that the function has three solutions when the restoring point is 0. Fig. 4(b) demonstrates the potential energy has double wells, in which the energy in the two external equilibrium points is the minimum and the potential energy of the middle equilibrium point is the maximum value.

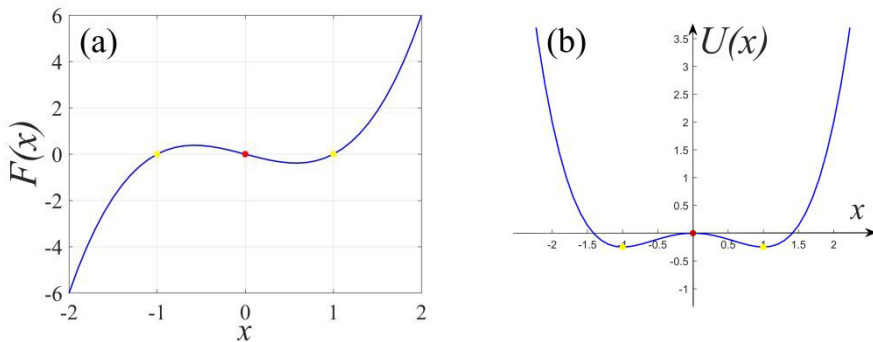


Fig. 4. The restoring force function curve (a) and the potential energy function curve (b) of the variable mass symmetric bistable nonlinear oscillator. (Red dots represent unstable static equilibrium points, and yellow dots represent stable static equilibrium points.)

Fig. 5 displays the displacement response, 3D diagram and phase diagram under three different excitation conditions with a step size of 0.01. From Fig. 5, we can see that the results of the two algorithms are in good agreement under the fixed step size. In addition, the calculation time in Table 2 shows that the Lie derivative algorithm is efficient at the same time step.

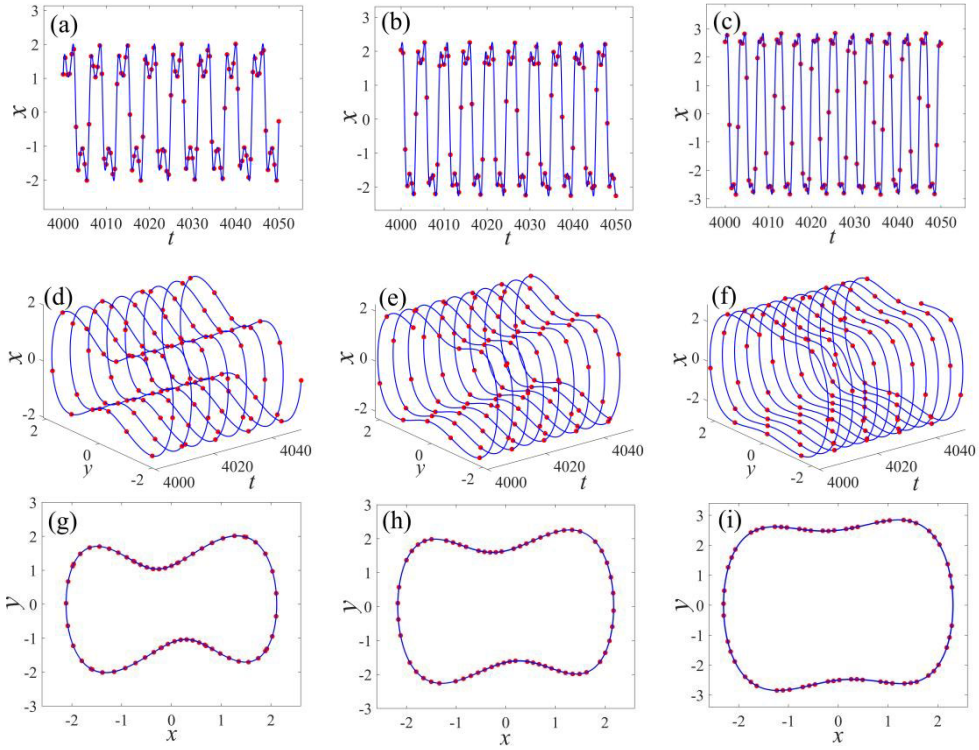


Fig. 5. The displacement response, 3D diagram, and phase diagram of the variable mass symmetric bistable nonlinear oscillator for (a, d, g) where $\omega = 1$, $f = 2$, (b, e, h) $\omega = 1.2$, $f = 2$, (c, f, i) where $\omega = 1.5$, $f = 2$ (The blue line is the calculation result of the Lie derivative algorithm, and the red point is the calculation result of the Runge-Kutta algorithm)

Fig. 6 describes the numerical results of these two algorithms in different step sizes, where the step size of Lie derivative discretization is 0.1, while the size of the Runge-Kutta algorithm has remained the same. It can be observed that the results of the two numerical algorithms with different step sizes are consistent, which further shows that the Lie derivative discretization algorithm has the characteristics of large step size. It demonstrates that the Lie derivative discretization algorithm has the ability to handle more extended step sizes.

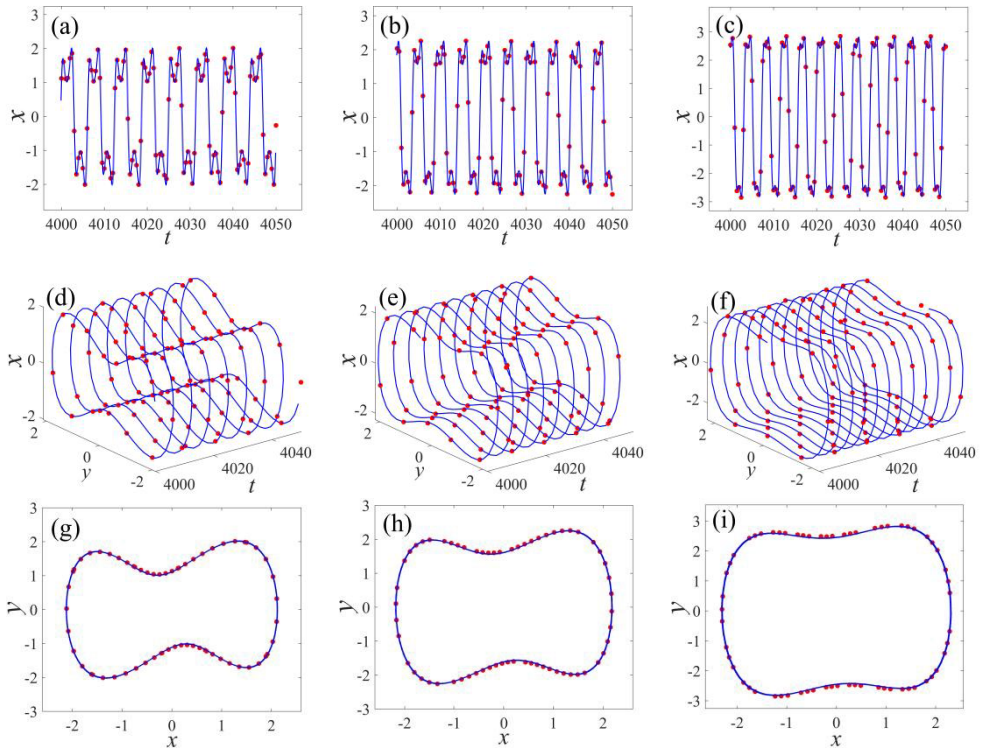


Fig. 6. The displacement response, 3D diagram, and phase diagram of the variable mass symmetric bistable nonlinear oscillator for (a, d, g) where $\omega = 1, f = 2$, (b, e, h) where $\omega = 1.2, f = 2$, (c, f, i) where $\omega = 1.5, f = 2$ (The blue line is the calculation result of the Lie derivative algorithm, and the red point is the calculation result of the Runge-Kutta algorithm).

Fig. Method	Fig.5(a)	Fig.5(b)	Fig.5(c)
Lie	0.1223	0.1450	0.1277
Ode45	1.8910	1.8537	2.0758

Table 2. The computational cost of the two numerical schemes from the system (8)

3.3 Variable mass asymmetric bistable nonlinear oscillator

In order to understand the numerical behavior of the proposed schemes, an asymmetric bistable nonlinear oscillator with variable mass is provided as

$$m_0(1 + \alpha t)\ddot{x}(t) + (m_0\alpha + c)\dot{x}(t) - x(t) + x^2(t) + x^3(t) = f \cos(\omega t) \tag{10}$$

Similarly, the second-order discretization can be derived

$$\begin{aligned} x_{k+1} &= x_k + hL_{g_1}^1(t_k, x_k, y_k) + \frac{h^2}{2}L_{g_1}^2(t_k, x_k, y_k), \\ y_{k+1} &= y_k + hL_{g_2}^1(t_k, x_k, y_k) + \frac{h^2}{2}L_{g_2}^2(t_k, x_k, y_k), \end{aligned} \quad (11)$$

where,

$$\begin{aligned} L_{g_1}^1(t_k, x_k, y_k) &= y_k, t_{k+1} = t_k + h, \\ L_{g_1}^2(t_k, x_k, y_k) &= -\frac{m_0\alpha + c}{m_0(1+\alpha t)}y_k + \frac{1}{m_0(1+\alpha t)}x_k - \frac{1}{m_0(1+\alpha t)}x_k^2 - \frac{1}{m_0(1+\alpha t)}x_k^3 + \frac{f \cos(\omega t)}{m_0(1+\alpha t)}, \\ L_{g_2}^1(t_k, x_k, y_k) &= -\frac{m_0\alpha + c}{m_0(1+\alpha t)}y_k + \frac{1}{m_0(1+\alpha t)}x_k - \frac{1}{m_0(1+\alpha t)}x_k^2 - \frac{1}{m_0(1+\alpha t)}x_k^3 + \frac{f \cos(\omega t)}{m_0(1+\alpha t)}, \\ L_{g_2}^2(t_k, x_k, y_k) &= \left[\frac{1}{m_0(1+\alpha t)} - \frac{2}{m_0(1+\alpha t)}x_k - \frac{3}{m_0(1+\alpha t)}x_k^2 \right] y_k - \frac{m_0\alpha + c}{m_0(1+\alpha t)}L_{g_2}^1(t_k, x_k, y_k). \end{aligned}$$

In a similar way to plot the restoring force and potential energy function curves, it can be confirmed from Fig. 7 that the system is asymmetric and bistable.

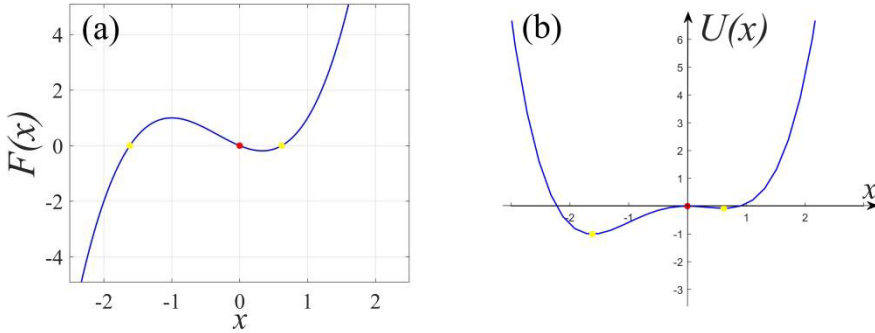


Fig. 7. The restoring force function curve (a) and the potential energy function curve (b) of the variable mass asymmetric bistable nonlinear oscillator. (Red dots represent unstable static equilibrium points, and yellow dots represent stable static equilibrium points.)

Fig. 8 compares the Lie derivative numerical algorithm and the fourth-order Runge-Kutta algorithm with a step size of 0.01. The contrast diagram verifies the correctness of the discretization algorithm of the Lie derivative. In addition, it can be seen from Table 3 that using the Lie derivative discretization algorithm can shorten the calculation time and improve the calculation efficiency.

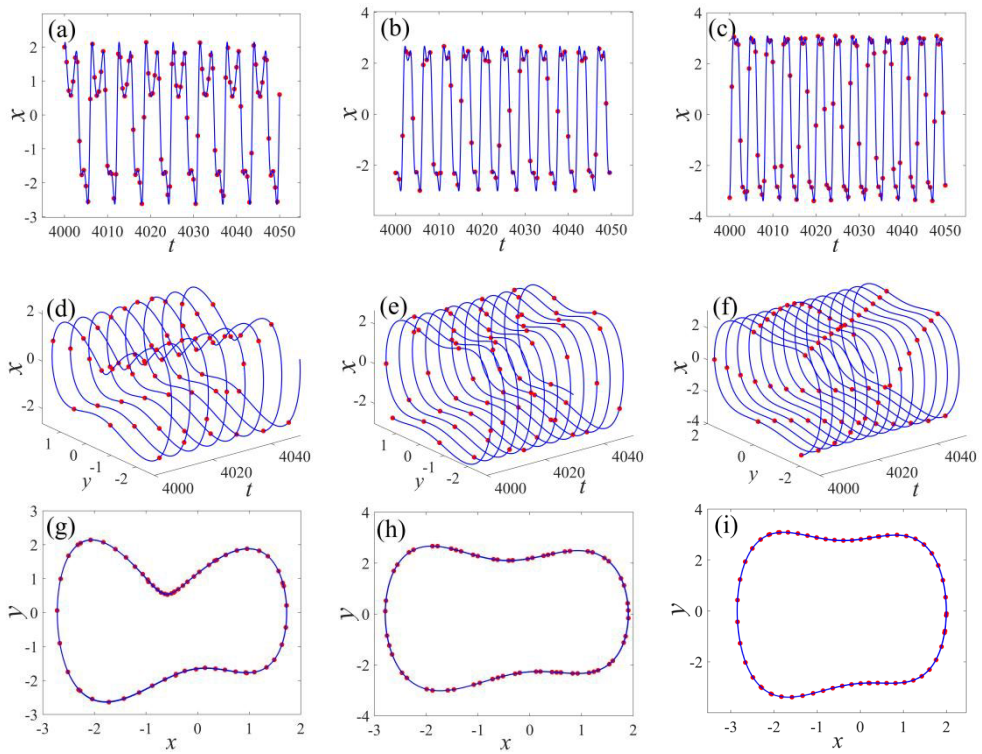


Fig. 8. The displacement response, 3D diagram, and phase diagram of the variable mass asymmetric bistable nonlinear oscillator for (a, d, g) where $\omega = 1.2, f = 1$, (b, e, h) where $\omega = 1.5, f = 1$, (c, f, i) where $\omega = 1.7, f = 1$ (The blue line is the calculation result of the Lie derivative algorithm, and the red point is the calculation result of the Runge-Kutta algorithm).

Fig. 9 presents the dynamical response of the Lie derivative algorithm and the Runge-Kutta methods, in which the step size of the Lie derivative scheme is 0.1, and the step size of the Runge-Kutta algorithm is 0.01. From the comparison, it can be concluded that when the step size of the Lie derivative discretization numerical algorithm increases, the calculation results can still get desirable solutions, which proves that it has the characteristics of a large step size.

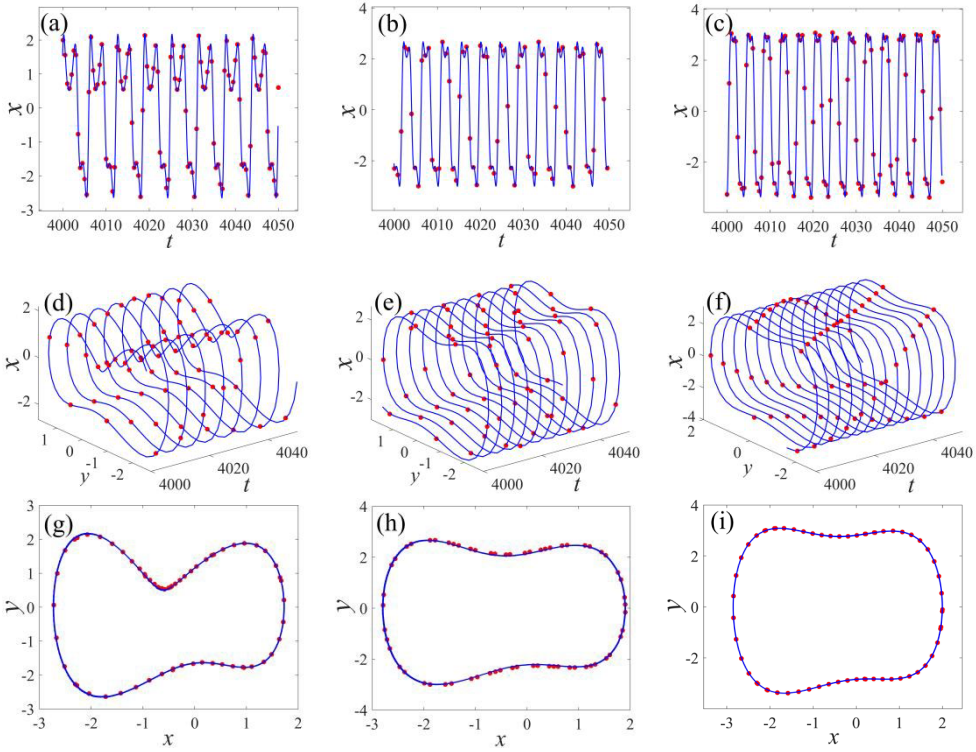


Fig. 9. The displacement response, 3D diagram, and phase diagram of the variable mass asymmetric bistable nonlinear oscillator for (a, d, g) where $\omega = 1.2, f = 1$, (b, e, h) where $\omega = 1.5, f = 1$, (c, f, i) where $\omega = 1.7, f = 1$ (The blue line is the calculation result of the Lie derivative algorithm, and the red point is the calculation result of the Runge-Kutta algorithm).

Fig. Method	Fig.8(a)	Fig.8(b)	Fig.8(c)
Lie	0.1309	0.1333	0.1336
Ode45	1.9739	1.9862	1.9963

Table 3. The computational cost of the two numerical schemes from the system (10)

3.4 Variable Mass Linear Oscillator

Finally, a variable mass linear oscillator is examined, and its control equation is given by

$$m_0(1 + \alpha t)\ddot{x}(t) + (m_0\alpha + c)\dot{x}(t) + x(t) = f \cos(\omega t) \quad (12)$$

With the help of formula (3), the discrete iteration formulas are given by

$$\begin{aligned} x_{k+1} &= x_k + hL_{g_1}^1(t_k, x_k, y_k) + \frac{h^2}{2}L_{g_1}^2(t_k, x_k, y_k), \\ y_{k+1} &= y_k + hL_{g_2}^1(t_k, x_k, y_k) + \frac{h^2}{2}L_{g_2}^2(t_k, x_k, y_k), \end{aligned} \quad (13)$$

where,

$$L_{g_1}^1(t_k, x_k, y_k) = y_k, t_{k+1} = t_k + h,$$

$$L_{g_1}^2(t_k, x_k, y_k) = -\frac{m_0\alpha + c}{m_0(1 + \alpha t)} y_k - \frac{1}{m_0(1 + \alpha t)} x_k + \frac{f \cos(\omega t)}{m_0(1 + \alpha t)},$$

$$L_{g_2}^1(t_k, x_k, y_k) = -\frac{m_0\alpha + c}{m_0(1 + \alpha t)} y_k - \frac{1}{m_0(1 + \alpha t)} x_k + \frac{f \cos(\omega t)}{m_0(1 + \alpha t)},$$

$$L_{g_2}^2(t_k, x_k, y_k) = -\frac{1}{m_0(1 + \alpha t)} y_k - \frac{m_0\alpha + c}{m_0(1 + \alpha t)} L_{g_2}^1(t_k, x_k, y_k).$$

We plot the dynamical responses of the variable mass linear oscillator with $h = 0.01$ for both the Lie derivative algorithm and the Runge-Kutta methods in Fig. 10, which indicates that the outcome of the Lie derivative discretization algorithm is consistent with those of the Runge-Kutta algorithm. In addition, it can be seen from Table 4 that the computation time of the Lie derivative discretization algorithm is significantly shortened, which proves that the algorithm is efficient.

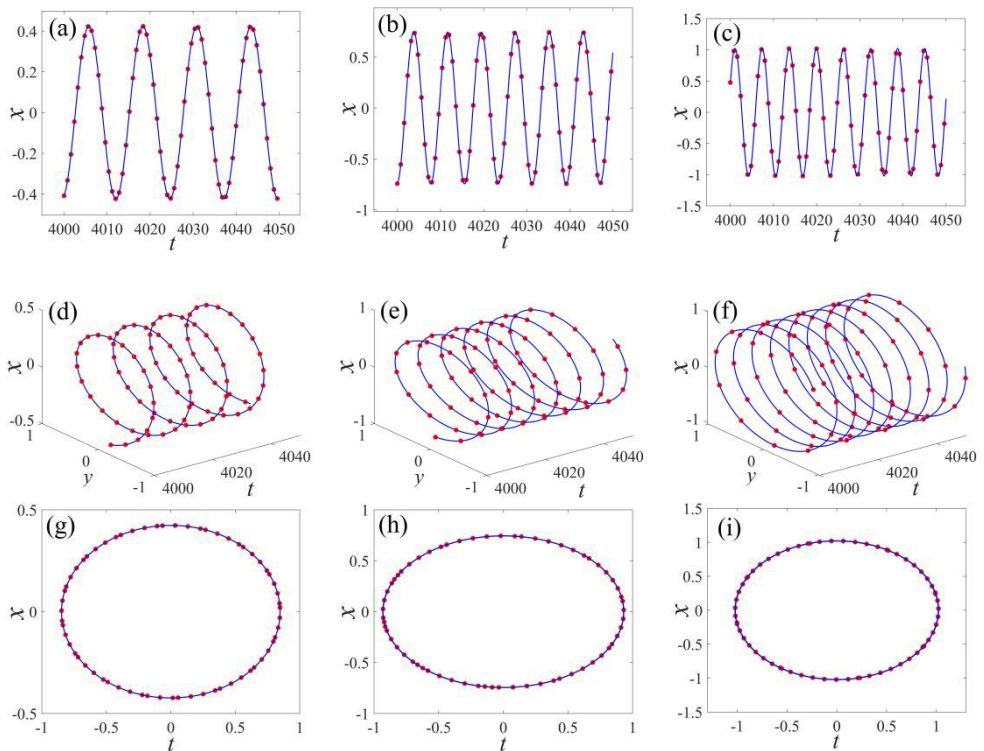


Fig. 10. The displacement response, 3D diagram, and phase diagram of the variable mass linear oscillator for (a, d, g) where $\omega = 0.5, f = 0.8$, (b, e, h) where $\omega = 0.8, f = 0.8$, (c, f, i) where $\omega = 1, f = 0.8$ (The blue line is the calculation result of the Lie derivative algorithm, and the red point is the calculation result of the Runge-Kutta algorithm).

Meanwhile, we also plot the response curves with different time steps for these two methods in Fig. 11, where the time step of Lie derivative discretization is assigned as 0.1, while the Runge-Kutta algorithm is 0.01. It can be found that both these schemes produce similar outcomes. It

demonstrates that the Lie derivative discretization algorithm possesses the qualities of a long stage.

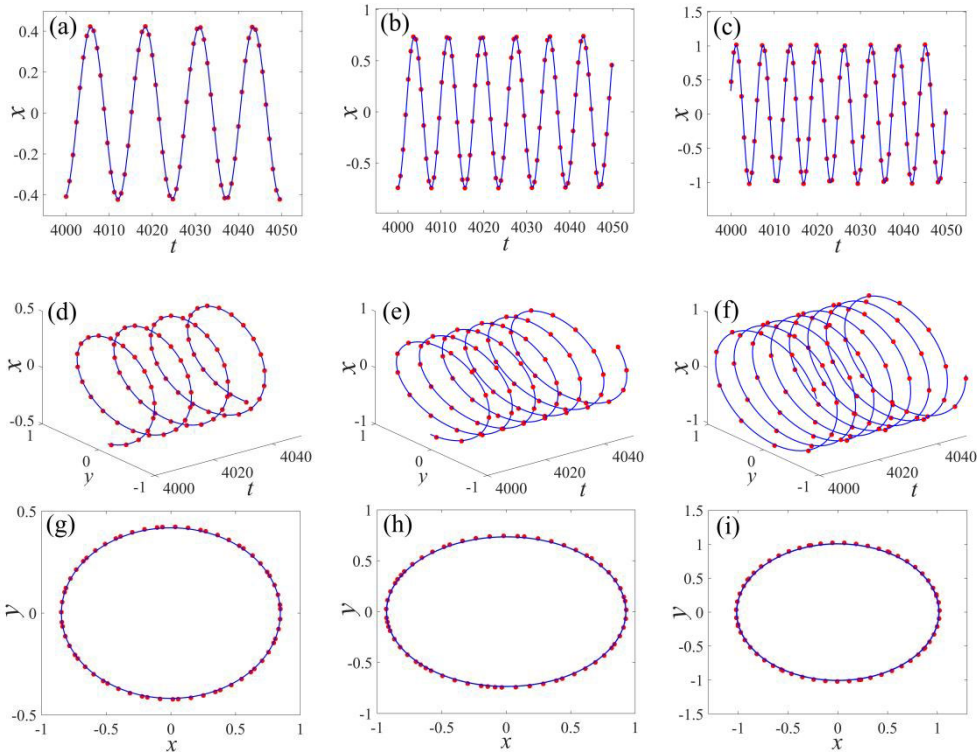


Fig. 11. The displacement response, 3D diagram, and phase diagram of the variable mass linear oscillator for (a, d, g) where $\omega = 0.5, f = 0.8$, (b, e, h) where $\omega = 0.8, f = 0.8$, (c, f, i) where $\omega = 1, f = 0.8$ (The blue line is the calculation result of the Lie derivative algorithm, and the red point is the calculation result of the fourth-order Runge-Kutta algorithm).

Fig. Method	Fig.10(a)	Fig.10(b)	Fig.10(c)
Lie	0.0620	0.0625	0.0636
Ode45	1.7836	1.9172	1.7824

Table 4. The computational cost of the two numerical schemes from the system (12)

4. Conclusions

This paper extends an algorithm for variable mass systems by using Lie derivative expansion. Four variable mass oscillators were taken as numerical experiments to evaluate the efficiency and precision of the proposed methods. The accuracy of the Lie derivative discretization algorithm is verified by comparing with the fourth-order Runge-Kutta method. The time history curves and the phase portraits are plotted, and the computational cost of the CPU is remarked. The numerical

calculations demonstrate the remarkable efficiency of the Lie derivative discretization algorithm for solving variable mass systems. It is also found that the algorithm can get consistent solutions under a large time step, which proves that the Lie derivative discretization algorithm has the merit of short calculation time.

Acknowledgements: The authors are supported by the National Natural Science Foundation of China (Nos. 12232009 and 12472001), and the General Scientific Research Project of Liaoning Province (No. LJKZ0089).

References:

- Cao Z, Kang H, Liu H, et al. (2023). Modeling and dynamic response of variable mass system of maglev turning electric spindle, *Nonlinear Dynamics*, 111 (1), 255-274.
- Chen W, Chen G, Chen T, et al. (2024). Dynamic response analysis of a typical time-varying mass system: A moving-interface pipe model, the WKB-recursive solution and experimental validation, *Appl. Math. Model.*, 125, 147-166.
- Cveticanin L (2001). Dynamic buckling of a single-degree-of-freedom system with variable mass, *Eur. J. Mech A-Solid.*, 20 (4), 661-672.
- Cveticanin L (2012). A review on dynamics of mass variable systems, *J. Serbian Soc. Comput. Mech.*, 6, 56-73.
- Cveticanin L (2016). *Dynamics of Bodies with Time-Variable Mass*, Springer, Basel.
- Flores J, Solovey G, Gil S (2003). Variable mass oscillator, *Am. J. Phys.*, 71 (7), 721-725.
- Gouin H (2023). Remarks on the Lie derivative in fluid mechanics, *Int. J. Non-Linear Mech.*, 150, 104347.
- Hurtado J E (2018). Analytical dynamics of variable-mass systems, *J. Guid. Control. Dynam.*, 41 (3), 701-709.
- Irschik, Hans, Holl H J (2004). Mechanics of variable-mass systems-part 1: balance of mass and linear momentum, *Appl. Mech. Rev.*, 57 (2), 145-160.
- Iavernaro F, Mazzia F, Mukhametzhanov M S, Sergeev Ya D (2021). Computation of higher order Lie derivatives on the Infinity Computer. *J. Comput. Appl. Math.*, 383, 113135.
- Letellier C, Mendes E M, Mickens R E (2007). Nonstandard discretization schemes applied to the conservative Hénon-Heiles system, *Int. J. Bifurcat. Chaos.*, 17 (3), 891-902.
- Meena G D, Janardhanan S (2018). Taylor-Lie formulation based discretization of nonlinear systems, *Int. J. Dynam. Control.*, 6, 459-467.
- Mendesa E M, Billings S A (2002). A note on discretization of nonlinear differential equations, *Chaos*, 12 (1), 66-71.
- Mendes E, Letellier C (2004). Displacement in the parameter space versus spurious solution of discretization with large time step, *J. Phys. A: Math. Gen.*, 37 (4), 1203-1218.
- Monaco S, Normand-Cyrot D, A combinatorial approach of the nonlinear sampling problem. In: 9th Int. Conf. Analysis and Optimization of Systems, (1990) June 12-15, Antibes, France, *Lecture Notes in Control and Information Sciences*, Vol. 144, 20 pp., 788-797.
- Nhleko S (2009). Free vibration states of an oscillator with a linear time-varying mass, *J. Vib. Acoust.*, 145 (6), 051011.
- Zhang X, Li H, et al (2022). Exploiting multiple-frequency bursting of a shape memory oscillator, *Chaos. Solitons, Fractals.*, 158, 112000.